NOTCH3 SIGNALING REGULATES MUSASHI-1 EXPRESSION IN METASTATIC COLORECTAL CANCER CELLS.

NOTCH3 Signaling Regulates MUSASHI-1 Expression in Metastatic Colorectal Cancer Cells

Anna Pastò[1], Valentina Serafin[1], Giorgia Pilotto[2], Claudia Lago[2], Chiara Bellio[1],Livio Trusolino[3,4], Andrea Bertotti[3,4], Timothy Hoey[5], Michelina Plateroti[6], Giovanni Esposito[2], Marica Pinazza[1], Marco Agostini[1], Donato Nitti[1], Alberto Amadori[1,2], and Stefano Indraccolo[2]

Author Affiliations

[1]Department of Surgery, Oncology and Gastroenterology, University of Padova; [2]Istituto Oncologico Veneto IRCCS, Padova; [3]IRCC, Institute for Cancer Research and Treatment, Candiolo; [4]Department of Oncology, University of Torino School of Medicine, Torino, Italy; [5]OncoMed Pharmaceuticals Inc., Redwood City, California; and [6]Centre de Génétique et de Physiologie Moléculaire et Cellulaire, Université Claude Bernard Lyon 1, Villeurbanne, France

Author Notes

Current address for V. Serafin: Onco-hematology Laboratory, Department of Woman and Child Health, University of Padova, Padova, Italy.

Corresponding Author:

Stefano Indraccolo, Istituto Oncologico Veneto IRCCS, via Gattamelata, 64 Padova 35128, Italy. Phone: 0039-049-8215875; Fax: 0039-049-8072854; E-mail:stefano.indraccolo@unipd.it

[1]A. Pastò, V. Serafin, A. Amadori, and S. Indraccolo contributed equally to this work.

Abstract

MUSASHI-1 (MSI-1) is a well-established stem cell marker in both normal and malignant colon cells and it acts by positively regulating the NOTCH pathway through inactivation of NUMB, a NOTCH signaling repressor. To date, the mechanisms of regulation of MSI-1 levels remain largely unknown. Here, we investigated the regulation of MSI-1 by NOTCH signaling in colorectal cancer cell lines and in primary cultures of colorectal cancer metastases. Stimulation by the NOTCH ligand DLL4 was associated with an increase of MSI-1 mRNA and protein levels, and this phenomenon was prevented by the addition of an antibody neutralizing NOTCH2/3 but not NOTCH1. Moreover, forced expression of activated NOTCH3 increased MSI-1 levels, whereas silencing of NOTCH3 by short hairpin RNA reduced MSI-1 levels in both colorectal cancer cells and CRC tumor xenografts. Consistent with these findings, enforced NOTCH3 expression or stimulation by DLL4 increased levels of activated NOTCH1 in colorectal cell lines. Finally, treatment of colorectal cancer cells with anti-NOTCH2/3 antibody increased NUMB protein while significantly reducing formation of tumor cell spheroids. This novel feed-forward circuit involving DLL4, NOTCH3, MSI-1, NUMB, and NOTCH1 may be relevant for regulation of NOTCH signaling in physiologic processes as well as in tumor development. With regard to therapeutic implications, NOTCH3-specific drugs could represent a valuable strategy to limit NOTCH signaling in the context of colorectal cancers overexpressing this receptor.

Introduction

The NOTCH pathway is involved in intercellular communication and it regulates homeostasis of several tissues by controlling self-renewal, apoptosis, differentiation, and proliferation of cells (1). In mammals, NOTCH signals through four different receptors (NOTCH1–4) and five different ligands [JAGGED 1–2, Delta-like (DLL)-1, -3, and -4]. Binding of a ligand triggers a proteolytic cascade that ultimately leads to the release of the intracellular domain (ICD) of the NOTCH receptor. ICD migrates to the nucleus and interacts with the transcriptional complex C protein-binding factor

1/Suppressor of Hairless/Lag 1 (CSL), converting it from a transcriptional repressor to a transcriptional activator; this eventually translates into increased transcription of target genes, including members of the HES and HEY families (2). Increased NOTCH1 activity has been observed in various tumors (3), including intestinal tumors, where it is partially accomplished by β-catenin–mediated upregulation of the NOTCH ligand JAGGED-1 (4).

Aside from ligands, NOTCH activity is positively regulated by MUSASHI-1 (MSI-1), an RNA-binding protein of 39 kDa belonging to a conserved family of neural RNA-binding proteins composed of two RNA recognition motifs. MSI-1 binds the 3'-untranslated region of *NUMB*, thus repressing its translation (5). NUMB is a membrane-associated negative regulator of NOTCH signaling, which induces endosome-mediated degradation of NOTCH ICD, thus preventing its transmigration to the nucleus and eventual signaling (6). NUMB involvement in asymmetric cell division is well established: amounts of NUMB and levels of NOTCH signaling are heterogeneous in daughter cells and this tunes cell differentiation versus stem cell maintenance (7).

MSI-1 was initially recognized as an RNA-binding protein required for asymmetric cell division of sensory organ precursor cells in *Drosophila* (8). MSI-1 was also proposed to be required for asymmetric distribution of intrinsic determinants in the development of mammalian nervous system; indeed, its expression is enriched in undifferentiated neuronal precursors or neuronal stem cells (9). Moreover, MSI-1$^+$ cells were found in the mouse small intestine (10) and in the human colon at the base of the crypt compartment, where stem cells are considered to reside (11, 12), thus indicating that MSI-1 could label colon stem cells. Remarkably, despite its relevance for key physiologic processes, the mechanisms of regulation of MSI-1 levels remain largely unknown.

We recently demonstrated that NOTCH3 levels are significantly upregulated in primary and metastatic colorectal cancer samples compared with normal mucosa (13). Moreover, we also observed that a highly tumorigenic phenotype of colorectal cancer cells in xenograft models was associated with increased expression of various components of the NOTCH pathway. Forced expression of the active form of NOTCH3 mirrored the effects of DLL4 stimulation and promoted tumor formation (13), supporting an oncogenic role for NOTCH3 in colorectal cancer cells. In addition, recent evidence from the literature demonstrated upregulation of MSI-1 expression in both primary tumors and metastatic colorectal cancer samples, compared with normal colon tissue (14).

Stimulated by the above observations, we sought to investigate whether NOTCH signaling could regulate MSI-1 levels in tumor cells. We found that MSI-1 expression is induced by DLL4 stimulation through a mechanism involving NOTCH3. In turn, increased MSI-1 levels sustain NOTCH1 signaling by repressing NUMB. These observations highlight a novel feed-forward loop of regulation of NOTCH activity in cancer cells.

Materials and Methods

Cell lines, primary samples, and in vitro culture

Human liver metastasis samples were obtained from 25 patients bearing colon or rectal cancer following informed consent. Immediately after resection, tissues were washed in cold PBS containing penicillin/streptomycin (500 U/mL), gentamicin (1 μL/mL), and amphotericin (1.25 μg/mL). Samples were processed as described elsewhere (12). Briefly, the tissue was minced and incubated for 3 hours at 37°C with collagenase (1.5 mg/mL) and hyaluronidase (20 μg/mL; both from Sigma-Aldrich) in Dulbecco's Modified Eagle Medium (DMEM)/F12 medium (Gibco, Invitrogen). The digested material was centrifuged and sequentially filtered through 70 μm mesh; red blood cell lysis was performed at 37°C for 7 minutes in $NH_4Cl/KHCO_3$/EDTA buffer and cell viability assessed by Trypan Blue dye exclusion. Before experimental use, cells were resuspended in DMEM/F12 medium and maintained at 37°C in a 5% CO_2 humidified atmosphere in low-adhesion plates for 1 week.

LoVo is a colorectal cancer cell line derived from a metastatic nodule from the supraclavicular region (15), whereas MICOL-14^{tum} is a tumorigenic variant of MICOL-14, a cell line derived from a lymph node metastasis of rectal cancer (16). The MICOL-14^{tum} cell line was established from a tumor developed in nonobese diabetic severe combined

immunodeficient (NOD/SCID) mice after subcutaneous injection of parental MICOL-14 cells in Matrigel plus angiogenic factors (17). The cells were grown in RPMI-1640 medium (Invitrogen) supplemented with 10% fetal calf serum (FCS; Gibco, Invitrogen) and 1% FCSL-glutamine and used within 6 months from thawing and resuscitation.

To stimulate NOTCH signaling, P12 wells were coated with soluble recombinant human DLL4 (hDLL4, 4 μg/mL; R&D Systems) in PBS/0.1% bovine serum albumin (BSA, Sigma-Aldrich). One day later, MICOL-14^{tum}, LoVo cells, or primary cultures from tumor samples were added at a density of 2×10^5 cells per well in RPMI-1640 medium supplemented with 10% FCS and 1% L-glutamine (Invitrogen) and cultured for 72 hours before analysis. The monoclonal antibodies (mAb), including anti-NOTCH1 (OMP-52M51), anti-NOTCH2/3 (OMP-59R5), and the control antibody (OMP-1B711), developed by OncoMed Pharmaceuticals Inc. in collaboration with MorphoSys AG (Martinsried, Germany; ref. 18) were used at 10 μg/mL final concentration.

Flow cytometry (FACS) analysis

After 72 hours of treatment, the cells were collected and incubated with Live/Dead dye (Invitrogen) for 30 minutes at 4°C to stain dead cells. After washing in PBS, cells were fixed in 4% paraformaldehyde and permeabilized with 0.1% Triton X-100. Nonspecific binding was prevented by saturation with PBS/5% BSA, followed by incubation with rabbit anti-human MSI-1 (1:200; Abcam) or mouse anti-human MUC-1 (1:100; Abcam) mAb. Cells were then stained with the appropriate secondary antibodies (Alexa 1:500; Invitrogen) and analyzed by fluorescence-activated cell sorting (FACS; LSR II, BD Biosciences). Aldehyde dehydrogenase (ALDH) enzyme activity in viable cells was determined by a fluorogenic dye (Aldefluor assay, Stem Cell Technologies) according to the manufacturer's instructions. Briefly, 1×10^6/mL cells were suspended in Aldefluor assay buffer containing ALDH substrate (Bodipy-Aminoacetaldehyde) and incubated for 45 minutes at 37°C. As a control, cells were suspended in buffer containing Aldefluor substrate in the presence of diethylaminobenzaldehyde, a specific ALDH enzyme inhibitor. Data were collected from at least 5×10^4 cells per sample on live cell gate and analyses performed with Flow Jo (TreeStar).

RNA extraction, reverse transcription, and quantitative PCR analysis

Total RNA was extracted from cell populations by TRIzol (Invitrogen) according to the manufacturer's instructions. cDNA was synthesized from 0.5–1 μg of total RNA using the Superscript II reverse transcriptase (Invitrogen). Fifty-five nanograms of cDNA were used as a template and mixed with 10 μL of 2× Platinum SYBR Green qPCR SuperMix-UDG (Invitrogen) and primers (Supplementary Table S1) in a reaction volume of 20 μL. Cycling conditions were 10 minutes at 95°C, 60 cycles of 15 seconds at 95°C, and 1 minute at 60°C. Each sample was run in duplicate on ABI PRISM 7900HT Sequence Detection System (PE Biosystems). Results were analyzed using the comparative $\Delta\Delta C_t$ method: data are presented as the fold difference in gene expression normalized to the housekeeping gene β_2-microglobulin and relative to a relevant reference sample. Quantitative reverse transcriptase (qRT)-PCR efficiency was in the range 95%–105%.

Western blotting

After 72 hours of treatment, the cells were harvested, lysed, and subjected to SDS-PAGE and Western blotting. The membrane was saturated with PBS 5% nonfat dry milk (Sigma-Aldrich) for 1 hour at room temperature. Immunoreactivity was evaluated by hybridization using the following antibodies: rabbit anti-MSI-1 (1:1,000 final dilution; Abcam), rabbit Anti-NUMB (1:500 final dilution; Millipore), rabbit anti-NOTCH1 ICD (1:1,000, final dilution; Val 1744, Cell Signaling Technology), and mouse anti-α-tubulin mAb (1:5,000 final dilution; Sigma-Aldrich). The blots were then hybridized with a 1:5,000 dilution of horseradish peroxidase-conjugated anti-mouse or anti-rabbit antibody (Amersham-Pharmacia). Finally, chemiluminescence was detected by SuperSignal kit (Pierce).

Transduction of cells with viral vectors

Lentiviral vectors encoding short hairpin RNA (shRNA) targeting human *NOTCH3* (sh235, sh238) or a scrambled shRNA as a control were purchased from Sigma-Aldrich and used as previously reported (13). The N3 ΔE retroviral vector, encoding constitutively active forms of human *NOTCH3* and the control MX vector have been described elsewhere (19). The *NOTCH2*-ICD-encoding retroviral vector pMSVpuroICN2 was a kind gift of Adolfo Ferrando (Columbia University,

New York, NY). The human DLL4-EGFP and the control retroviral construct lacking DLL4 have been previously described (20). Vector stocks were generated by a transient three-plasmid vector packaging system, as previously described (21). For transduction of MICOL-14^{tum} and LoVo cells, 200 µL of concentrated vector-containing supernatant were layered over target cells, previously seeded into 12-well culture plates at 1 × 10^5 cells per well. After 6–9 hours at 37°C, the supernatant was replaced with 2 mL complete medium. Assessment of transgene expression was performed 72 to 96 hours after transduction.

In vivo experiments and optical imaging of tumor

NOD/SCID mice were purchased from Charles River. Procedures involving animals and their care were performed according to institutional guidelines that comply with national and international laws and policies (EEC Council Directive 86/609, OJ L358, 12 December 1987). Implantation and expansion of CRC358 and CRC149 patient-derived tumor xenografts were performed as previously described (22, 23). Established tumors (average volume 500 mm^3) were treated with a control mAb or with the anti-NOTCH2/3 mAb (40 mg/kg) by intraperitoneal injection every 2 weeks. Tumor size was evaluated once-weekly by caliper measurements and the approximate volume of the mass was calculated using the formula $4/3\pi \times (d/2)^2 \times D/2$, where d is the minor tumor axis and D is the major tumor axis. When tumor volume reached 2,500 mm^3, mice were sacrificed by cervical dislocation; tumors were harvested by dissection and subjected to flow cytometry analysis or fixed in formalin and embedded in paraffin (FFPE) for histologic analysis.

To establish MICOL-14^{tum} xenografts, 5 × 10^5 tumor cells were resuspended in PBS and subcutaneously injected in dorsolateral flanks of NOD/SCID mice, as previously reported (13). Before injection, MICOL-14^{tum} cells were transduced by a lentiviral vector encoding the *luciferase* gene. Anti-NOTCH2/3 mAb was administered by intraperitoneal injection (40 mg/kg) the day following tumor cell injections and every 2 weeks thereafter. Bioluminescence signals were acquired on IVIS Imaging System (Xenogen Corporation) as described elsewhere (24).

Histology and immunohistochemical analysis

Quantification of necrosis was carried out after hematoxylin/eosin staining by a light microscope equipped with digital camera and MODEL software (Leica Microsystems). Immunohistochemistry (IHC) was performed on FFPE samples using a standard avidin-biotin immunoperoxidase complex technique (Dako, Milano, Italy). Four-µm-thick sections were mounted on silanized slides, dewaxed in xylene, dehydrated in ethanol, boiled in 0.01 M citrate buffer (pH 6.0) for 15 min in a microwave oven (95°C), and incubated with 3% hydrogen peroxide for 5 min. After washing with PBS, samples were incubated in PBS/10% BSA for 30 min, followed by overnight incubation at 4°C with rabbit anti MSI-1 antibody (1:100; Abcam). Sections were subsequently incubated with biotinylated goat anti-rabbit immunoglobulin (Vectastain ABC kit, Vector Lab., Burlingame, CA) and peroxidase-conjugated avidin (Dako). Lastly, 0.02% diaminobenzidine and 1% hydrogen peroxide (Dako) in PBS were used as substrates in the color development reaction. Sections were then counterstained with hematoxylin. Immunoreactivity was scored for both the intensity and the percentage of marker-positive cells: intensity was given scores 0 to 3 (no staining = 0, light staining = 1, moderate staining = 2, and strong staining = 3) and percentage was given scores 1 to 6 (0%–4% = 1, 5%–20% = 2, 21%–40% = 3, 41%–60% = 4, 61%–80% = 5, and 81%–100% = 6). Finally, the two scores were multiplied to obtain the final score ranging from 0 to 18.

Immunofluorescence analysis

MICOL-14^{tum} cells were plated on poly-D-lysine-coated glasses at 5 × 10^4 cells/spot, fixed in 4% paraformaldehyde and permeabilized with 0.1% Triton X-100. Nonspecific binding was prevented by incubation in PBS 5% BSA for 1 h. Staining was carried out by incubating cells with anti-MSI-1 (1:100; Abcam) mAb for 90 min, anti-CK18 (1:200; Abcam) mAb and anti-NOTCH1 ICD (1:800; Abcam) mAb for 30 min at room temperature. After three washes in PBS, appropriate secondary Alexa-conjugated antibodies (1:500; Molecular Probes, Invitrogen) were added for 1 h. Nuclear staining was performed by Topro-3 incubation (1:1,000; Invitrogen) for 10 min. The cells were finally washed twice with PBS and mounted in glycerol. Confocal laser scanning microscopy was carried out with a Zeiss LSM 510 microscope (Zeiss, Jena, Germany) using Argon (488 nm) and Helium-Neon (543–633 nm) laser sources. Stained cells were analyzed by

laser scanning microscopy. Data from 5 different fields for each section were used to calculate mean fluorescence intensity.

Statistical analysis

Data of replicate experiments were shown as mean values ± Standard Deviation (SD). Comparisons between groups were made by the Student *t* test.

Further experimental details are available in the Supplementary Data.

Results

hDLL4 upregulates MSI-1 transcript levels in CRC cells by a NOTCH2/3-mediated mechanism

We preliminarily established conditions for ligand-mediated stimulation of NOTCH signaling in CRC cells. To this end, MICOL-14^{tum} cells transfected with the CSL-luc plasmid were stimulated by hDLL4 and NOTCH activity measured by *in vitro* luciferase reporter assay 72 h later. An 8-fold increase in luciferase activity was observed in hDLL4-stimulated cells, compared with basal levels (Supplementary Fig. S1A). Importantly, these effects were blocked by anti-NOTCH2/3 but not by anti-NOTCH1 mAb (Supplementary Fig. S1A). Because MICOL-14^{tum} cells express NOTCH1–3 but lack NOTCH4 receptors (13), we could conclude that DLL4 stimulation triggers NOTCH signaling mainly through NOTCH2 and/or NOTCH3. These data were also supported by measurement of endogenous components of the NOTCH pathway by qRT-PCR. Indeed, in 5 independent experiments, stimulation of MICOL-14^{tum} cells with hDLL4 increased *NOTCH3* and *HEY-2* transcript levels by 5- to 8-fold, and this effect again was blocked by anti-NOTCH2/3 mAb (Supplementary Fig. S1B). Similar effects were observed in primary cultures derived from CRC metastases (n = 4); as shown in Supplementary Fig. S1C, *NOTCH-3* and *HEY-2*transcript levels were significantly increased after hDLL4 stimulation and markedly decreased in the presence of anti-NOTCH2/3. At variance with MICOL-14^{tum} cells, incubation of primary tumor cells with anti-NOTCH2/3 significantly reduced levels of all*NOTCH*-related transcripts tested (including *NOTCH1–3*, *HES-1* and *HEY-2*) also in the absence of hDLL4 stimulation. Moreover, in primary samples hDLL4 increased levels of all components of the NOTCH pathway tested (including *NOTCH2, NOTCH3*, *HES-1* and*HEY-2*), but not *NOTCH1* (Supplementary Fig. S1C).

Next, we investigated the effects of DLL4 stimulation on the expression of stem cell–associated and differentiation markers. We observed that recombinant hDLL4 induced a 2- to 3-fold increase in *MSI-1* levels in MICOL-14^{tum} cells, which was largely blocked by anti-NOTCH2/3 treatment (Fig. 1A). We also observed increased levels of *MUCIN-1* (*MUC-1*) and *MUCIN-2* (*MUC-2*) mRNA following NOTCH2/3 blockade in cultures analyzed (Fig. 1A). Because MUC-1 is a marker of secretory goblet cells (25), this finding supports previous observations indicating that NOTCH2/3 prevents colon progenitors from differentiating into secretory cells (26). In contrast, only marginal changes in *NUMB*transcripts were detected in these experiments either in the presence or in the absence of hDLL4 (Fig. 1A). To extend these findings, we stimulated LoVo cells with hDLL4. In this case, however, only *MSI-1* mRNA levels increased significantly, whereas no changes were detected in *MUC-1*, *MUC-2* or *NUMB* levels (Fig. 1B). Moreover, treatment with anti-NOTCH 2/3 blocked the effects of hDLL4 on *MSI-1* levels, and increased *MUC-1* transcript levels (Fig. 1B)

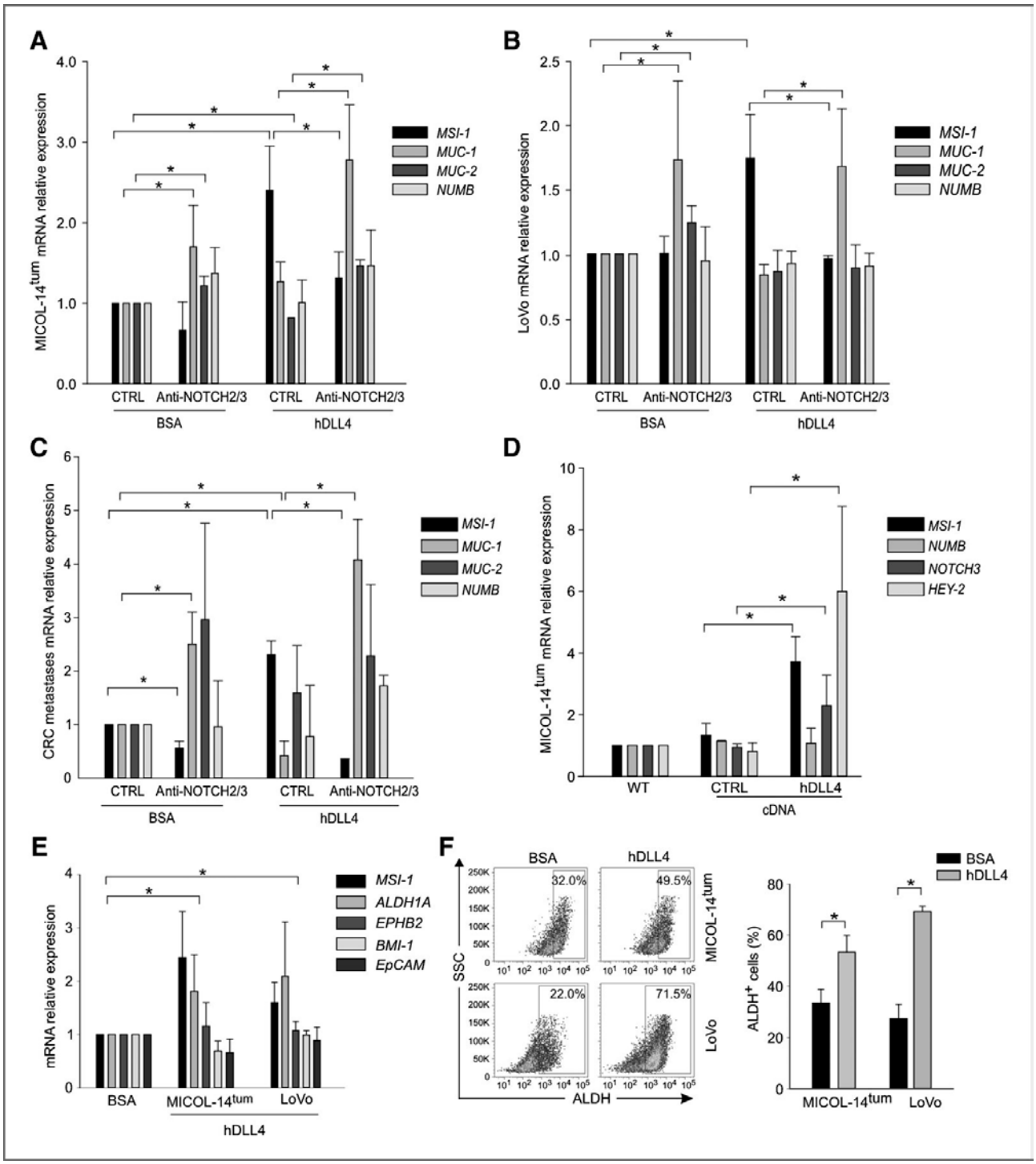

Figure 1.

hDLL4-mediated increase of MSI-1levels is counteracted by NOTCH2/3 blockade. A–C, measurement by qRT-PCR of genes associated with stemness (MSI-1, NUMB) or differentiation (Muc-1 and Muc-2) after 72-hour stimulation with hDLL4 in MICOL-14tum cells (A), LoVo cells (B), or primary cultures from CRC liver metastasis (C) in the presence of anti-NOTCH2/3 or control mAb. Data, mean ± SD of five (A) and four (B and C) different experiments. *, $P < 0.05$. D, qRT-PCR following forced expression of hDLL4 into MICOL-14tum cells. MSI-1, NOTCH3 as well as HEY-2 significantly increased, whereas no substantial alteration in NUMB RNA levels was detected compared with control (CTRL) or parental (WT) cells. Data, mean ± SD of three different replicates. *, $P < 0.05$. E, qRT-PCR of additional stemness markers in MICOL-14tum and LoVo cells after 72 hours of stimulation with hDLL4. MSI-1 is the only marker significantly increased by hDLL4; data, mean ± SD of three (LoVo) and four (MICOL-14tum) different experiments. *, $P< 0.05$. F, flow cytometry analysis of ALDH activity in MICOL-14tum and LoVo cells after stimulation with hDLL4. Gates are set on the isotype control and values indicate the percentage of ALDH+ cells. The histogram on the right represents the mean percentage ±SD of four experiments in MICOL-14tum and three experiments in LoVo cells.

Finally, hDLL4 led to increased *MSI-1* expression and to a corresponding decrease in*MUC-1* levels also in primary cultures derived from liver CRC metastases, whereas only marginal changes were detected in *MUC-2* and *NUMB* levels, and these modulations were completely blocked by anti-NOTCH2/3 (Fig. 1C). Of note, treatment of primary tumor cultures with anti-NOTCH2/3 was associated with a significant reduction of *MSI-1*expression and concomitant increase of *MUC-1* and *MUC-2* levels also in the absence of hDLL4 stimulation (Fig. 1C), probably reflecting higher endogenous levels of NOTCH signaling, compared with MICOL-14^{tum} cells.

Upregulation of *MSI-1* levels was also observed following retroviral vector-mediated delivery of hDLL4 cDNA in MICOL-14^{tum} cells (Fig. 1D), thus confirming results obtained with recombinant hDLL4. To test whether the effect of hDLL4 was restricted to *MSI-1*expression, we addressed mRNA levels of several stem cell–associated genes in MICOL-14^{tum} and LoVo cells after hDLL4 stimulation. As reported in Fig. 1E, DLL4 stimulation significantly increased *MSI-1* levels and a trend towards increased *ALDH1A* expression was detected, whereas *BMI-1*, *EpCAM* and *EPHB2* mRNA levels did not substantially change. Because it is reported that NOTCH signaling upregulates ALDH (27), we evaluated by flow cytometry ALDH activity in both MICOL-14^{tum} and LoVo cells. As reported in Fig. 1F, hDLL4 stimulation was followed by a significant increase in ALDH activity in both tumor cell lines.

Effect of NOTCH2/3 blockade on MSI-1 and NUMB protein levels in CRC cells

To corroborate these findings, we investigated MSI-1 expression at protein level in primary cultures of 5 liver CRC metastases by flow cytometry. As shown in Fig. 2A and B, increased numbers of MSI-1^{+} cells were found following hDLL4 stimulation; moreover, anti-NOTCH2/3 mAb strongly reduced the percentage of MSI-1^{+} cells in both hDLL4-stimulated and control cell cultures (Fig. 2A and B), whereas treatment with anti-NOTCH1 only had marginal effects on MSI-1 expression (Fig. 2A). Confocal immunofluorescence analysis confirmed that hDLL4 stimulation increased MSI-1 expression in MICOL-14^{tum} cells, and this effect was blocked by anti-NOTCH2/3 mAb (Fig. 2C). In contrast, the expression of CK18, a common epithelial marker for colon cancer cells, was not affected by these treatments (Fig. 2C). Notably, anti-NOTCH2/3 treatment markedly reduced MSI-1 protein levels also in the absence of hDLL4 stimulation (Fig. 2A–C), exceeding variations in *MSI-1*transcript levels seen under the same experimental conditions (Fig. 1B). Finally, we analyzed reciprocal effects of hDLL4 stimulation and anti-NOTCH2/3 blockade on NUMB protein levels by Western blotting. As shown in Fig. 2D, hDLL4 stimulation was associated with a small decrease in NUMB protein levels, whereas anti-NOTCH2/3 mAb clearly increased NUMB protein in both control and hDLL4-stimulated MICOL-14^{tum} and LoVo cells, as well as in primary tumor cell cultures (Fig. 2D). Notably, variations in NUMB protein levels were accompanied by minor changes in NUMB transcript levels (Fig. 1), in line with the idea that NUMB protein modulation could be accounted for by MSI-1, which mainly affects posttranscriptional mRNA processing (5).

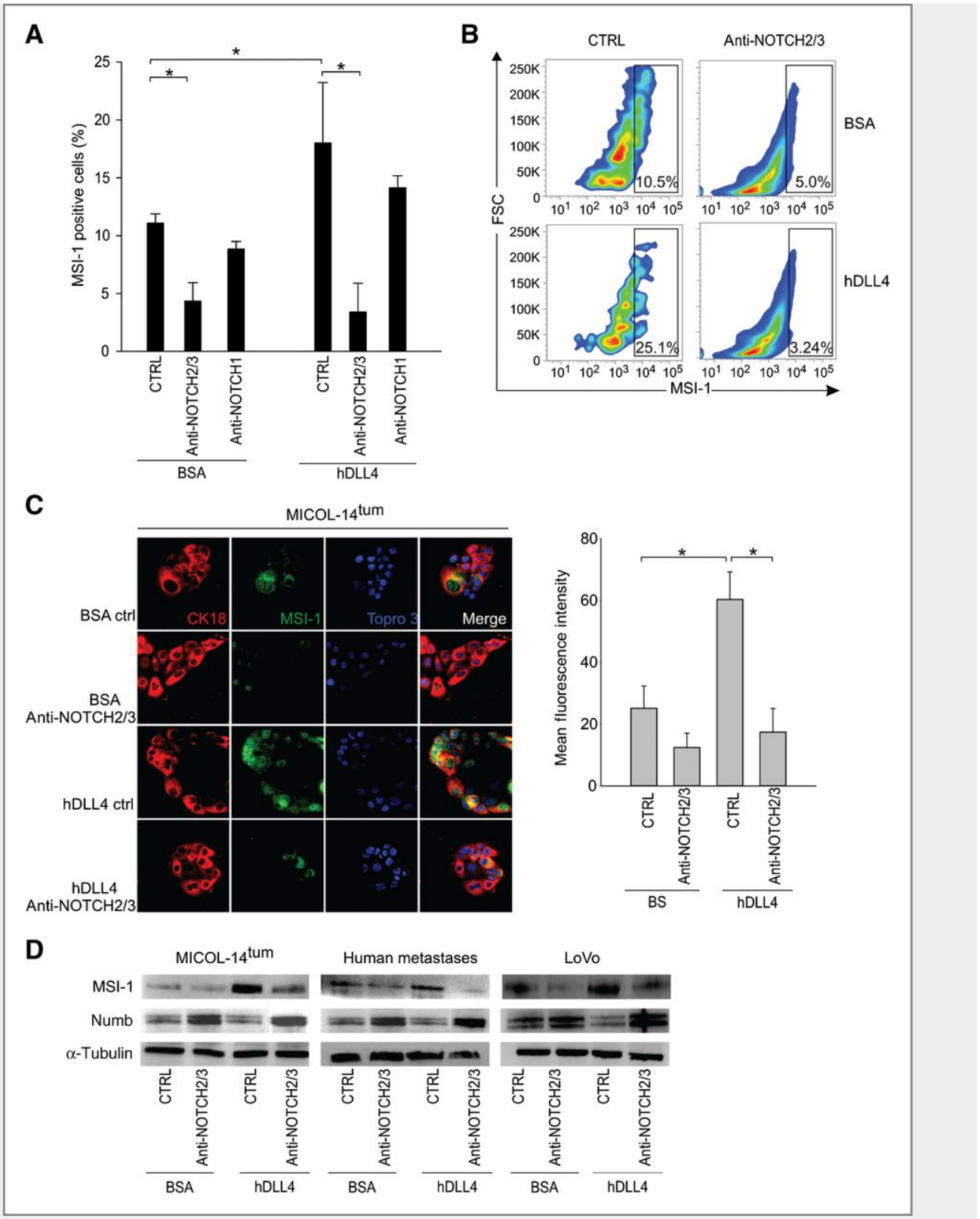

Figure 2.

NOTCH2/3-dependent increase of MSI-1 protein levels by hDLL4 in CRC cells. A, analysis of MSI-1 expression in primary cultures from liver CRC metastases cultured for 72 hours in hDLL4-coated wells (or BSA as a control) in the presence and in the absence of anti-NOTCH2/3, anti-NOTCH1, or control (CTRL) mAb. Data, mean ± SD of the percentage of MSI-1$^+$cells according to flow cytometric analysis (n = 3–5 experiments). *,$P < 0.05$. B, representative analysis of MSI-1 expression in a primary culture from a liver CRC metastasis. hDLL4 stimulation increased MSI-1 expression and this effect was completely blocked by anti-NOTCH2/3 mAb. Gates are set on the isotype control and values indicate the percentage of MSI-1$^+$ cells. C, on the left, immunofluorescence analysis of MSI-1 expression in MICOL-14^{tum}cells cultured for 72 hours in the presence of hDLL4 or BSA, with anti-NOTCH2/3 or a control

mAb. Nuclei were stained with TOPRO-3; the cytoplasm was stained with anti-CK18. Magnification, × 40. The histogram on the right represents mean fluorescence intensity for MSI-1 (488 channel) calculated as described in Materials and Methods. *, $P < 0.05$. D, Western blot analysis of MSI-1 and NUMB expression in CRC cells. Protein lysates were obtained from MICOL-14^{tum}, LoVo cells, and primary samples of CRC metastases cultured as described above; α-tubulin was used to normalize loading of the lanes. One representative experiment out of three is shown.

MSI-1 modulation is NOTCH-3 dependent

To clarify which NOTCH paralog mainly controls MSI-1 expression, we overexpressed either NOTCH3 (N3) or NOTCH2 (N2) ICD in MICOL-14^{tum} cells by using retroviral vectors. Forced N3ICD expression increased *MSI-1* levels by 3-fold, together with upmodulation of*HEY-2* levels (Fig. 3A). In contrast, overexpression of N2ICD increased *HEY-2* but caused minimal changes in *MSI-1* mRNA levels (Fig. 3A). These results were confirmed in LoVo cells, where forced N3ICD expression strongly increased *MSI-1, NOTCH3*, and *HEY-2*levels (Fig. 3B). Altogether, these results fit the hypothesis that hDLL4 could upregulate MSI-1 by a NOTCH3-mediated mechanism.

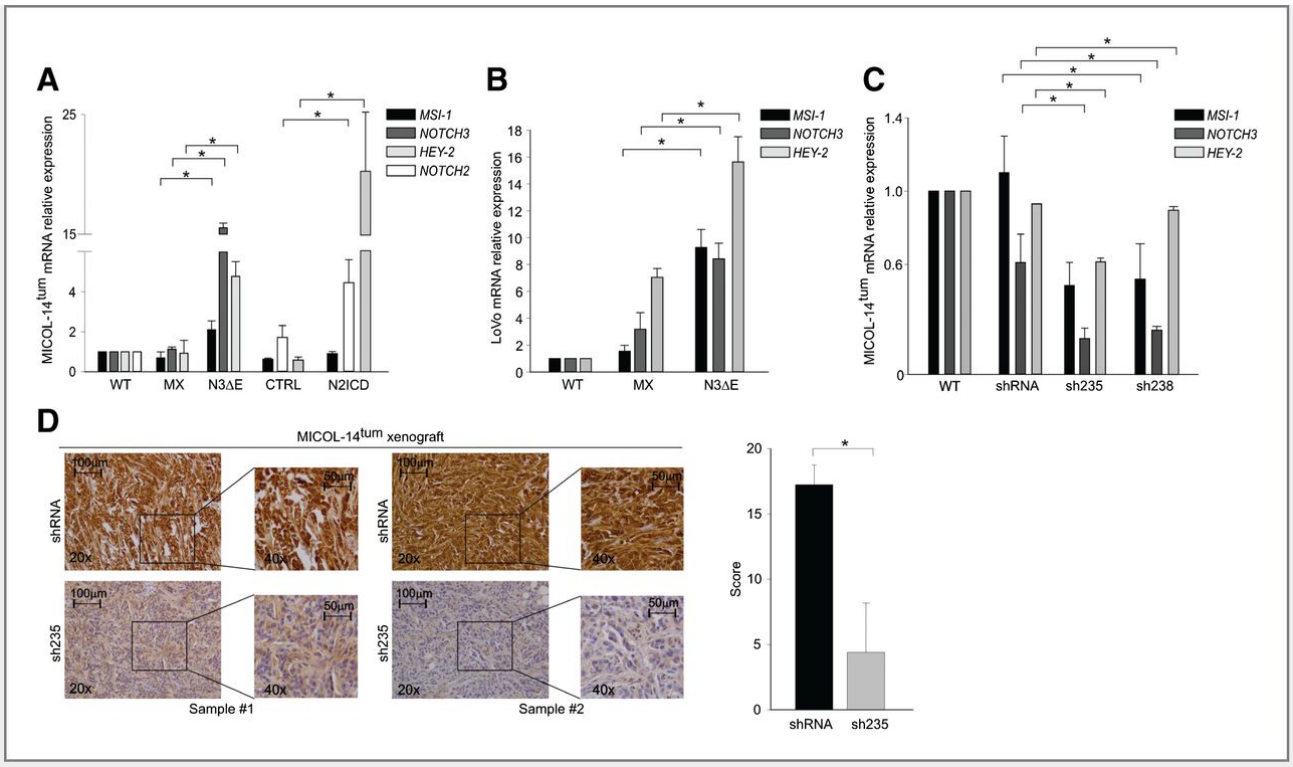

Figure 3.

NOTCH3 contributes to regulation of MSI-1 levels in CRC cells and patient-derived tumor xenografts. A and B, qRT-PCR after forced expression of activated *NOTCH3*(N3ΔE) or *NOTCH2* (N2ICD) into MICOL-14^{tum} (A) or LoVo (B) cells. The columns show relative levels of *NOTCH2, NOTCH3, MSI-1*, and *HEY-2* transcripts. Data, mean ± SD of three different replicates. *, $P < 0.05$. C, qRT-PCR after shRNA-mediated *NOTCH3* silencing (sh235, sh238) in MICOL-14^{tum}. *NOTCH3*, *HEY-2*, and *MSI-1* levels were significantly decreased compared with control vector (shRNA) or parental (WT) cells. Data, mean ± SD of three different replicates. *, $P < 0.05$. D, immunohistochemical analysis of MSI-1 expression in tumor xenografts formed by MICOL-14^{tum} cells bearing attenuated levels of *NOTCH3* expression (sh235) or control cells (shRNA) in NOD/SCID mice. Two different samples per group are shown at a ×20 and ×40 magnification. Columns show mean ±SD score of $n = 4$ samples, calculated as detailed in Materials and Methods.

As a complementary approach, *MSI-1* expression was investigated in MICOL-14^{tum} cells transduced by lentiviral vectors encoding *NOTCH3*-specific shRNA (sh235 and sh238). In agreement with our previous findings (13), *NOTCH3* silencing resulted in 40% to 60% decrease in *NOTCH3* mRNA levels (Fig. 3C), compared with control shRNA cells; in addition, significantly lower levels of *MSI-1* and *HEY-2* were recorded upon *NOTCH3*silencing, compared with control cells (Fig. 3C). In line with these *in vitro* findings, immunohistochemical analysis demonstrated very low MSI-1 expression in xenotransplanted tumors generated by MICOL-14^{tum} cells with attenuated NOTCH3 levels (Fig. 3D). Moreover, treatment of MICOL-14^{tum} xenografts with anti-NOTCH2/3 mAb caused a small but significant reduction of tumor burden measured

by optical imaging (Fig. 4A), associated with marked reduction of MSI-1 expression, increased MUC-1 levels (Fig. 4B) and reduction of cell proliferation, measured by Ki67 staining (Fig. 4C).

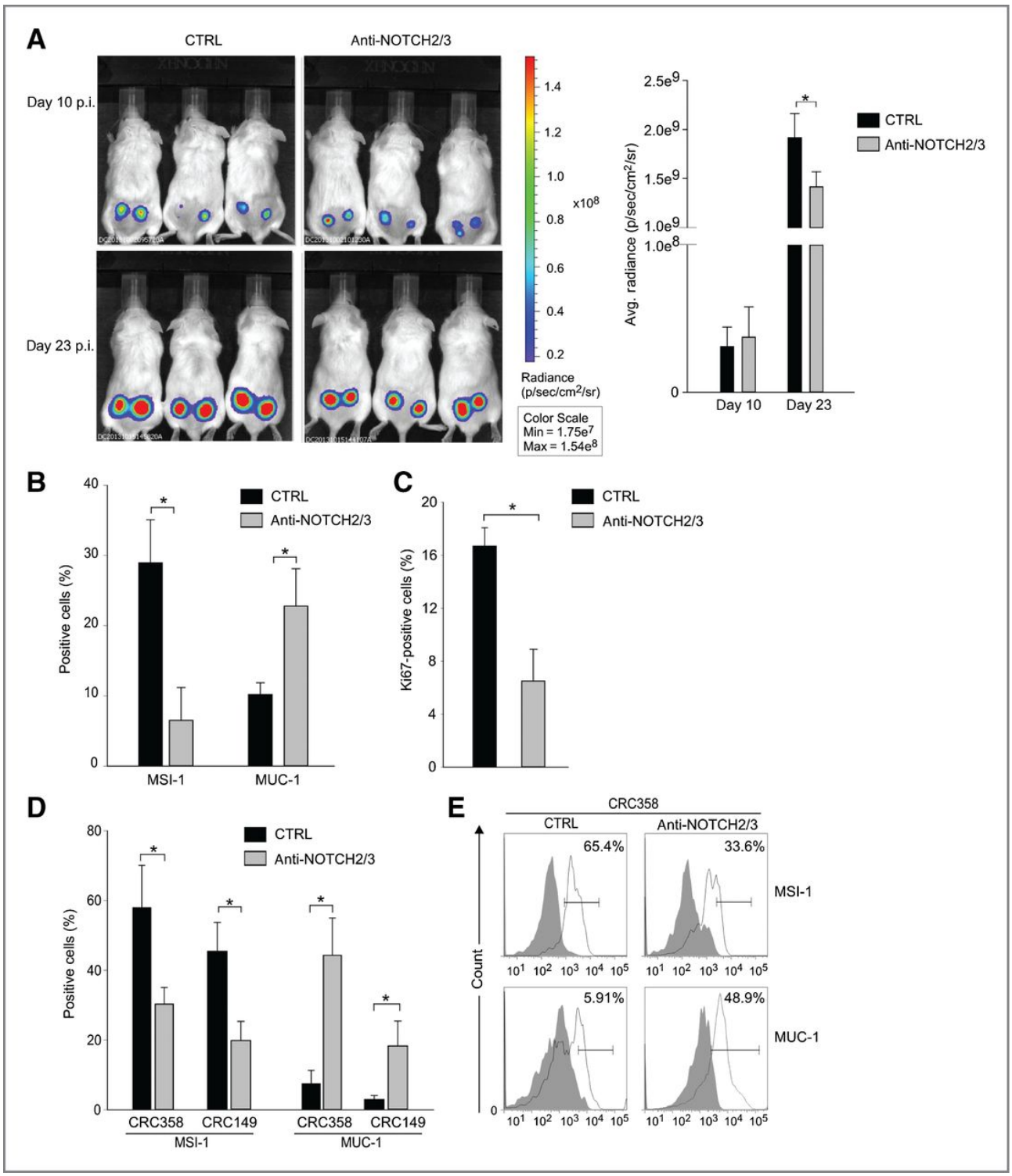

Figure 4.

NOTCH3 blockade affects MSI-1 and MUC-1 expression in CRC xenografts. A, optical imaging of subcutaneous tumors formed by MICOL-14^{tum} cells labeled with the luciferase gene. Left, representative images acquired at day 10 and 23 after tumor cell injection of three representative control (CTRL) or anti-NOTCH2/3-treated mice. Mice were treated with anti-NOTCH2/3 (OMP-59R5) or control antibody (OMP-1B711), both dosed at 40 mg/kg, at day 0 and day 14. Right, quantitative analysis of luciferase activity expressed as mean ± SD of 10 tumors per group showing significant reduction of tumor burden in anti-NOTCH2/3–treated mice. *, $P < 0.05$. B, modulation of MSI-1 and MUC-1 expression in tumor samples from anti-NOTCH2/3–treated or control mice by flow cytometry; columns indicate mean ± SD of the percentage of MSI-1$^+$ or MUC-1$^+$ cells (n = 10 samples/group). *, $P < 0.05$. C, reduced Ki67

expression in tumor samples from anti-NOTCH2/3–treated compared with control mice by flow cytometry; columns indicate mean ± SD of the percentage of Ki67$^+$ cells (n = 10 samples/group). *, $P < 0.05$. D, validation of results in patient-derived xenografts. MSI-1 and MUC-1 expression was analyzed by flow cytometry in xenografts obtained following subcutaneous injection of CRC 358 or CRC 149 cells into NOD/SCID mice and treatment with anti-NOTCH2/3 or control mAb of established tumors as detailed in Materials and Methods. Columns indicate mean ± SD of the percentage of MSI-1$^+$ or MUC-1$^+$ cells (n = 4 samples/group). *, $P < 0.05$. E, left, representative flow cytometry analysis of MSI-1 and MUC-1 expression in tumor samples. Filled peaks represent the isotype control and empty peaks indicate the percentage of MSI-1$^+$ or MUC-1$^+$cells.

To strengthen these findings, we decided to further investigate the *in vivo* consequences of NOTCH3 inhibition on MSI-1 levels in patient-derived tumor xenografts. First, we mined gene expression data from a large collection of patient-derived xenografts of metastatic colorectal carcinomas (22) and identified two cases bearing high-level expression of*NOTCH3* transcript (CRC 358 and CRC 149). NOTCH3 overexpression was confirmed at the protein level (data not shown). Then, we treated mice bearing large CRC 358 and CRC 149 tumor xenografts (average size 500 mm^3) with the anti-NOTCH2/3 or a control mAb. Analysis of tumor samples by flow cytometry disclosed a strong reduction in MSI-1 levels compared with control tumors and a concomitant increase in MUC-1 expression (Fig. 4D and E). All the above findings indicate that attenuation of NOTCH3 signaling by shRNA or mAb administration decreases MSI-1 expression in tumor cells, both *in vitro* and *in vivo*.

Effects of NOTCH2/3 blockade on the ability to form spheroids

MSI-1 is a well-recognized colon stem cell marker (11, 12) and one of the canonical features of cancer stem cells is their ability to form spheroids when cultured under specific*in vitro* culture conditions. We thus wondered whether experimental reduction of MSI-1 expression could affect the number of spheroid-forming cells. To test this hypothesis, we performed an ELDA assay with primary tumor cultures in the presence or in the absence of anti-NOTCH2/3 mAb. As shown in Fig. 5A, the frequency of spheroid-forming cells was significantly reduced in the presence of the anti-NOTCH2/3 antibody from 1/738 to 1/239. Similar results were obtained for LoVo and MICOL-14^{tum} cells: the spheroid-forming cell frequency decreased significantly in the presence of anti-NOTCH2/3 antibody (Fig. 5A). These results seemed to indicate that NOTCH2/3 blockade could at least in part affect cancer stem cell properties by modulating MSI-1 expression. In fact, frequency of spheroid-forming cells was significantly increased following overexpression of activated NOTCH3 in MICOL-14^{tum} cells (Fig. 5B), whereas it decreased, albeit not attaining statistical significance (P = 0.075), following attenuation of NOTCH3 levels by shRNA. On the whole, these results strongly indicated that NOTCH3 levels could impact on the clonogenic potential of CRC cells.

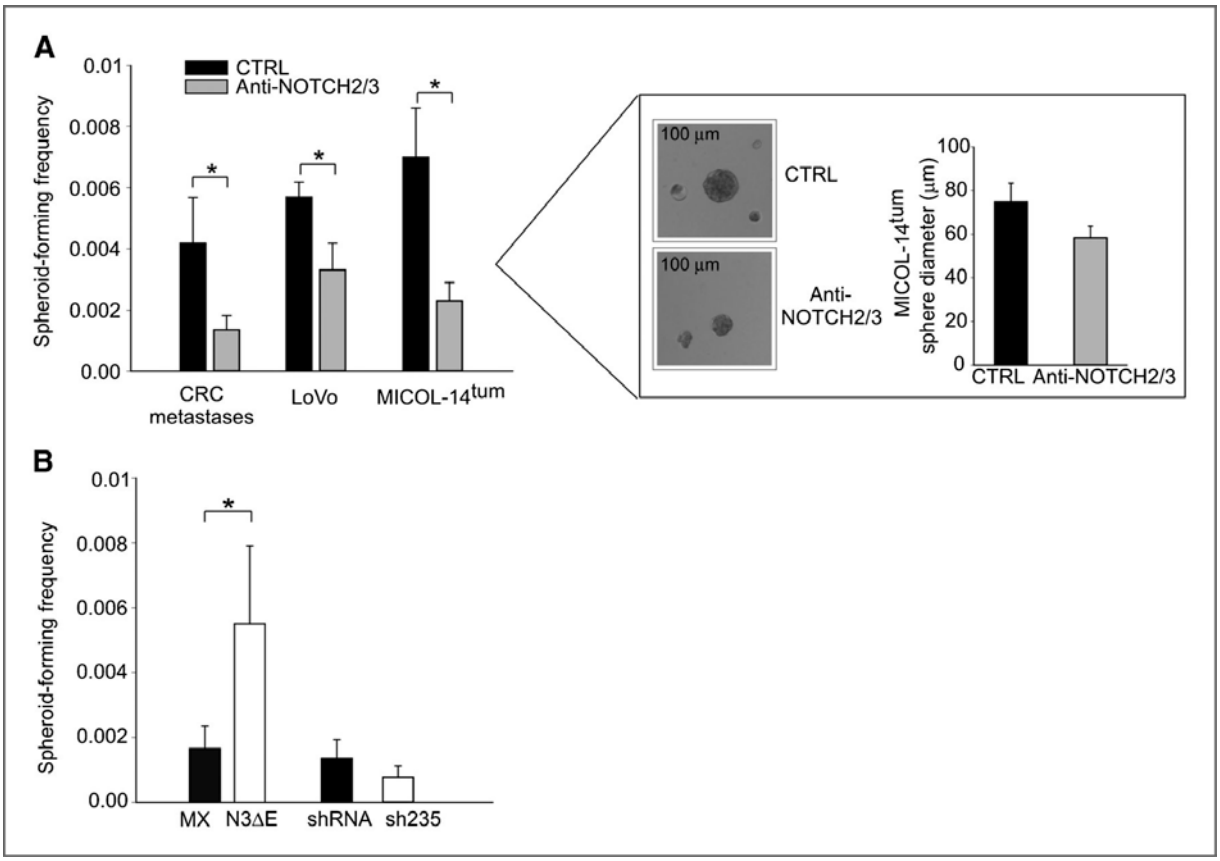

Figure 5.

Effects of NOTCH3 blockade on spheroid-forming ability. A, ELDA of MICOL-14^{tum}, LoVo cells, and primary cultures from CRC metastases. Cells were cultured at various concentrations for 4 days in the presence of anti-NOTCH2/3 or CTRL antibody. Data were analyzed by a specific web tool (as detailed in Materials and Methods) and expressed as mean values ± SD; *, $P < 0.05$. As shown in the box, spheroids obtained in the presence of anti-NOTCH 2/3 antibody were smaller than control spheroids, although the difference in spheroid diameter (~20%) was not statistically significant. B, ELDA of *NOTCH3*-overexpressing (N3ΔE) or control (MX), sh235- or shRNA- transduced MICOL-14^{tum} cells. The number of spheroid-forming cells was evaluated after 4 days in PhEMA-treated plates and analyzed by a specific web tool (as described in Materials and Methods); data, mean values ± SD. *, $P < 0.05$.

Effect of NOTCH3 modulation on NOTCH1 protein

Because NUMB is an established negative regulator of NOTCH1 ICD downstream of MSI-1 (21) and NOTCH3 regulates MSI-1 expression, we argued that NOTCH3 could indirectly behave as a regulator of activated NOTCH1 levels. Indeed, stimulation with hDLL4 was followed by increased nuclear levels of activated NOTCH1 in MICOL-14^{tum} cells (Fig. 6A), which are known to respond to hDLL4 stimulation mainly through NOTCH3 receptors (see Supplementary Fig. S1). Similar results were obtained following transfection of MICOL-14^{tum} cells with the N3ΔE (Fig. 6B). These results were further supported by Western blot analysis that disclosed a significant ($P = 0.002$) increase in N1ICD protein in MICOL-14^{tum}and LoVo cells overexpressing N3ΔE compared with controls (Fig. 5C; $n = 4$ independent experiments). Although *NOTCH3* is a recognized transcriptional target of NOTCH1 in certain cell types, this is the first direct evidence that NOTCH3 is part of a feed-forward circuit that stabilizes activated NOTCH1 in tumor cells.

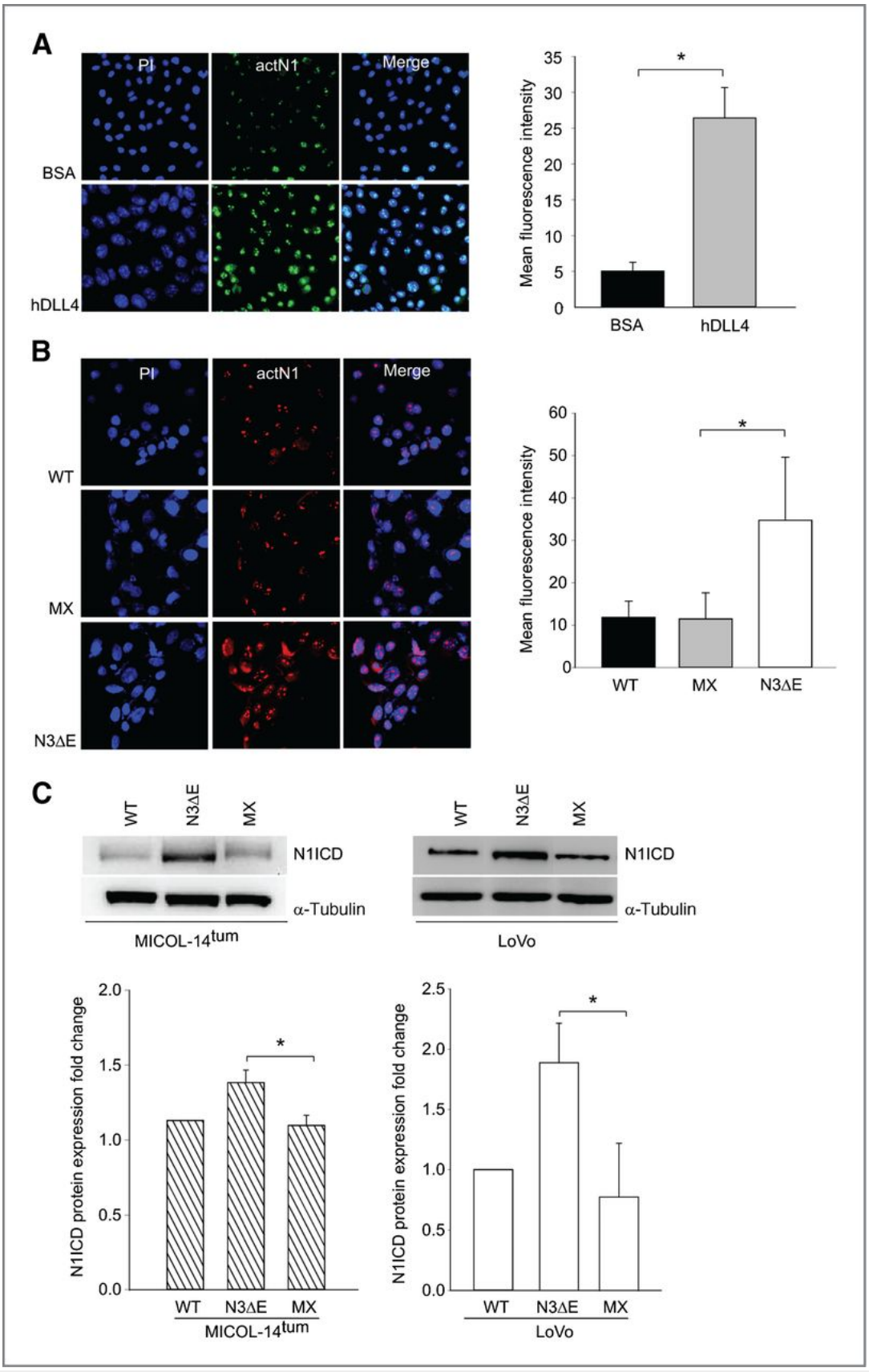

Figure 6.

NOTCH3 contributes to regulate NOTCH1 activity in CRC cells. A, immunofluorescence analysis of MICOL-14^{tum} cells cultured for 72 hours in hDLL4-coated wells reveals increased activated NOTCH1 levels (actN1) compared with control (BSA); nuclei were stained with TOPRO3. Magnification, × 20. Columns show mean fluorescence intensity of actN1 (488 channel), calculated as detailed in Materials and Methods. *, $P < 0.05$. B, immunofluorescence analysis of N1ICD expression in MICOL-14^{tum} cells transduced by a

retroviral vector encoding activated *NOTCH3*(N3ΔE); nuclei were stained with TOPRO3. Magnification, × 40. Columns show mean fluorescence intensity of actN1 (488 channel), calculated as detailed in Materials and Methods. *, $P < 0.05$. C, Western blot analysis of N1ICD expression in lysates of MICOL-14^{tum} (left) and LoVo cells (right) transduced by a vector encoding activated *NOTCH3* (N3ΔE), an empty vector (MIX) or parental cells (WT). One representative Western blot is shown in the top part of the panel. Columns report results of three independent experiments. *, $P < 0.005$.

Discussion

Although tumor cells often express multiple NOTCH paralogs, the reciprocal interplay between these receptors is not well understood. In T acute lymphoblastic leukemia (T-ALL), where activating mutations of NOTCH1 are common, NOTCH3 is considered as a canonical transcriptional target of NOTCH1 (28). Notably, NOTCH3 can also contribute to the oncogenic process in T-ALL, as shown by genetic studies in transgenic mice (29), although its transcriptional activity may be weaker compared with NOTCH1 due to the lack of the transactivation domain (30). In solid tumors, NOTCH3 signaling accounts for oncogenic features in breast (31), ovarian (32), lung (33), and colorectal cancer (13). However, as tumor samples often simultaneously coexpress NOTCH1 receptors, it is difficult to address the real contribution of NOTCH3 to NOTCH signaling in tumor cells. In particular, whether NOTCH3, in addition to its transcriptional activity on target genes shared with NOTCH1, could influence NOTCH1 signaling by other routes has not been as yet investigated.

In this work, based on the initial finding of increased MSI-1 levels in CRC cells after DLL4 stimulation, we postulate a possible novel mechanism of regulation of NOTCH1 activity by a feed-forward circuit involving NOTCH3 and MSI-1 (Fig. 7). MSI-1 is an RNA-binding protein that acts as a positive regulator of NOTCH activity by binding NUMB mRNA and blocking its translation, thus inhibiting NUMB-mediated degradation of NOTCH1 ICD. It is important to stress that NUMB regulates NOTCH1, but not NOTCH3 polyubiquitination in mammalian cells (34). On the basis of these data, variations in NUMB levels that we observed downstream of NOTCH3 are likely to impact on the accumulation of activated NOTCH1 but not NOTCH3 in tumor cells.

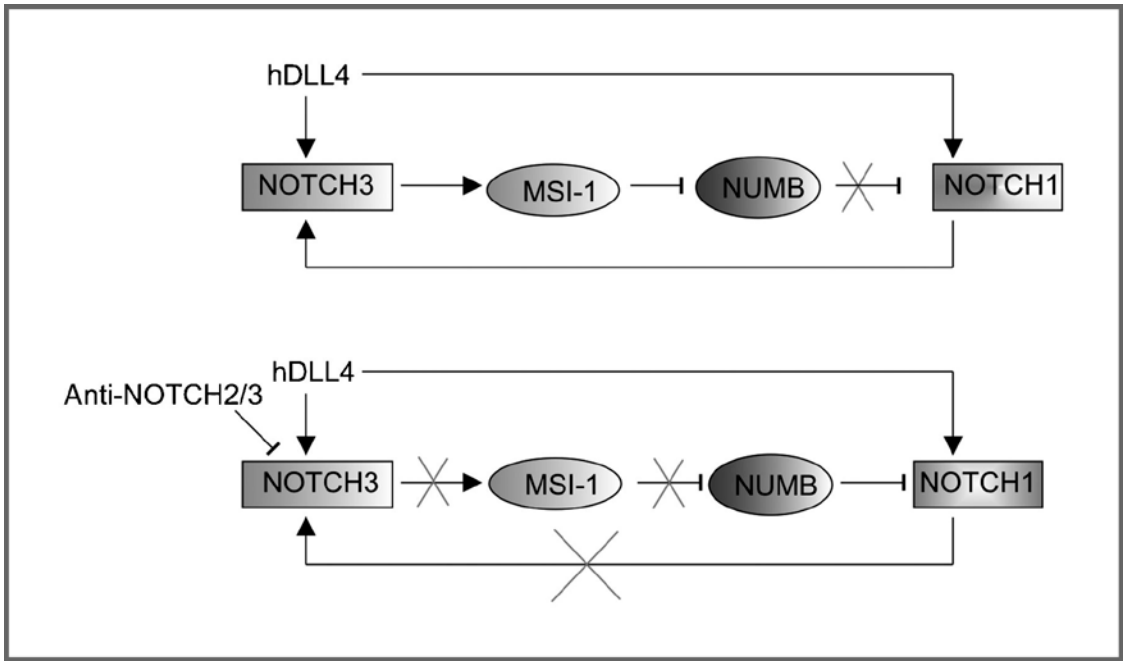

Figure 7.

A novel feed-forward circuit of regulation of NOTCH signaling in tumor cells. Top, triggering of the NOTCH3 receptor by DLL4 increases MSI-1 levels in CRC cells. This is followed by repression of NUMB-mediated inhibitory effects and increased NOTCH1 signaling. The mechanism can reinforce direct activation of NOTCH1 by DLL4. Activated NOTCH1 on its own further sustains transcription of NOTCH3, thus reinforcing the circuit. Bottom, inhibition of NOTCH3 (i.e., by neutralizing antibody) is one possibility of weakening NOTCH signaling by interfering with MSI-1–mediated effects.

Despite its established role in neural stem cells and as a marker of intestinal and mammary stem cells (9, 35), the molecular cues responsible for MSI-1 upregulation in cancer cells are largely unknown. In this study, by using complementary approaches (including loss-of-function experiments with neutralizing mAb or shRNA and gain-of-function experiments with retroviral vectors), we demonstrate for the first time that NOTCH3 affects MSI-1 levels in both tumor cell lines and primary tumor samples. In these latter, anti-NOTCH2/3 caused a significant attenuation of MSI-1 expression and a corresponding increase in MUC-1 levels also in the absence of DLL4 stimulation. This finding might reflect higher endogenous NOTCH activity in primary tumor cells compared with colon cancer cell lines, as previously observed by others (36). Although the experiments with anti-NOTCH2/3 mAb do not allow dissecting the contribution of these two receptors in the regulation of MSI-1 levels, the key role played by NOTCH3 is strongly supported by shRNA-mediated silencing of NOTCH3 in CRC cells, as well as by converse experiments (i.e., the experimental elevation of *NOTCH3*) and the lack of variations in*MSI-1* levels following forced *NOTCH2* ICD expression.

The mechanisms connecting NOTCH3 to MSI-1 remain as yet unknown. In any case, transfection of a plasmid bearing *MSI-1* promoter sequences upstream of the luciferase gene (37) into MICOL-14^{tum} cells overexpressing the activated *NOTCH3* did not result in increased luciferase activity compared with control cells (Supplementary Fig. S2). Moreover, bioinformatics analysis did not disclose classic CSL consensus binding sequences in the promoter region of *MSI-1* (not shown), nor was the *MSI-1* promoter found among genes bound by the active *NOTCH3* complex in ChIP-on-ChIP studies in ovarian cancer cells (38). Altogether, these results suggest that NOTCH3 could modulate MSI-1 levels by indirect mechanisms. In this regard, it was recently observed that several tumor suppressor microRNA (miR) act as direct regulators of *MSI-1*, affecting its expression pattern during tumorigenesis of brain tumors (39), opening the possibility that NOTCH3 controls *MSI-1* expression by miR-mediated mechanisms. To test this hypothesis, future studies will address whether miRs involved in the regulation of *MSI-1* are downstream on NOTCH3 in CRC cells.

Previous studies focusing on NUMB have revealed a reciprocal negative regulation between NOTCH and NUMB. In fact, it was shown that high levels of NOTCH signaling downregulate NUMB and NUMB-Like in mammalian cells (40). This phenomenon requires the PEST domain in the NUMB-like protein and it is blocked by the proteasome inhibitor MG132, eventually implying that it could be due to increased protein turnover. In that study, however, the possible contribution of NOTCH3 and MSI-1 to modulation of NUMB expression was not addressed. In our experiments, the reduction of *NUMB* is likely accounted for by the effects of MSI-1 on *NUMB* mRNA translation. These two complementary mechanisms converge on *NUMB* to keep its levels low under sustained NOTCH signaling. In addition to *NUMB*, MSI-1 has been shown to repress translation of mRNA encoding for the cell-cycle inhibitor p21^{waf} (41); therefore, in addition to NUMB, other MSI-1 targets could contribute to the biologic effects observed.

These findings may be of relevance for physiologic processes as well as for tumor development. In this respect, it is interesting to note that DLL4 stimulation was associated with markedly increased *ALDH1A* expression and ALDH activity. ALDH has been reported to be a specific marker for colon stem cells and it has been used to track stem cell populations during colon cancer development (42). These results confirm recent studies indicating that NOTCH signaling regulates ALDH activity both in normal stem cells and in cancer cells (27, 43, 44). With regard to therapeutic implications, whether anti-NOTCH3 therapy could be clinically effective by promoting differentiation of colorectal cancer cells possibly increasing their sensitivity to chemotherapy is an intriguing issue that deserves further investigation.

Disclosure of Potential Conflicts of Interest

No potential conflicts of interest were disclosed.

Authors' Contributions

Conception and design: A. Pastò, V. Serafin, D. Nitti, A. Amadori, S. Indraccolo

Development of methodology: A. Pastò, L. Trusolino

Acquisition of data (provided animals, acquired and managed patients, provided facilities, etc.): A. Pastò, G. Pilotto, C. Lago, C. Bellio, L. Trusolino, A. Bertotti, M. Plateroti, G. Esposito, M. Pinazza

Analysis and interpretation of data (e.g., statistical analysis, biostatistics, computational analysis): A. Pastò, V. Serafin, G. Pilotto, C. Lago, C. Bellio, A. Bertotti, M. Plateroti, G. Esposito, M. Pinazza

Writing, review, and/or revision of the manuscript: A. Pastò, V. Serafin, L. Trusolino, T. Hoey, A. Amadori, S. Indraccolo

Administrative, technical, or material support (i.e., reporting or organizing data, constructing databases): M. Agostini, S. Indraccolo

Grant Support

This work was supported by IG grants n. 14032 and n. 14295 from AIRC (A. Amadori and S. Indraccolo) and Fondazione Italiana per la Ricerca sul Cancro (FIRC); Ministry of University and Research, 60% and PRIN (A. Amadori), AIRC 2010 Special Program Molecular Clinical Oncology 5 × 1000, project 9970 (L. Trusolino); AIRC Investigator Grant 10116 (L. Trusolino); MIUR FIRB, Ministero dell'Università e della Ricerca, Fondo per gli Investimenti della Ricerca di Base—Futuro in Ricerca (A. Bertotti); American Association for Cancer Research—Fight Colorectal Cancer Career Development Award (A. Bertotti).

The costs of publication of this article were defrayed in part by the payment of page charges. This article must therefore be hereby marked *advertisement* in accordance with 18 U.S.C. Section 1734 solely to indicate this fact.

Acknowledgments

The authors thank Julien Nadjar for his help in transfection experiments.

References

1. Artavanis-Tsakonas S, Rand MD, Lake RJ. Notch signaling: cell fate control and signal integration in development. Science 1999;284:770–6.
2. Leong KG, Karsan A. Recent insights into the role of Notch signaling in tumorigenesis. Blood 2006;107:2223–33.
3. Miele L, Golde T, Osborne B. Notch signaling in cancer. Curr Mol Med2006;6:905–18.
4. Rodilla V, Villanueva A, Obrador-Hevia A, Robert-Moreno A, Fernandez-Majada V,Grilli A, et al. Jagged1 is the pathological link between Wnt and Notch pathways in colorectal cancer. Proc Natl Acad Sci U S A 2009;106:6315–20.
5. Moore MA. A cancer fate in the hands of a samurai. Nat Med 2010;16:963–5.
6. Kawahara H, Imai T, Imataka H, Tsujimoto M, Matsumoto K, Okano H. Neural RNA-binding protein Musashi1 inhibits translation initiation by competing with eIF4G for PABP. J Cell Biol 2008;181:639–53.
7. Imai T, Tokunaga A, Yoshida T, Hashimoto M, Mikoshiba K, Weinmaster G, et al. The neural RNA-binding protein Musashi1 translationally regulates mammalian numb gene expression by interacting with its mRNA. Mol Cell Biol 2001;21:3888–900.
8. Nakamura M, Okano H, Blendy JA, Montell C. Musashi, a neural RNA-binding protein required for Drosophila adult external sensory organ development. Neuron1994;13:67–81.
9. Okano H, Kawahara H, Toriya M, Nakao K, Shibata S, Imai T. Function of RNA-binding protein Musashi-1 in stem cells. Exp Cell Res 2005;306:349–56.
10. Potten CS, Booth C, Tudor GL, Booth D, Brady G, Hurley P, et al. Identification of a putative intestinal stem cell and early lineage marker; musashi-1. Differentiation2003;71:28–41.
11. Nishimura S, Wakabayashi N, Toyoda K, Kashima K, Mitsufuji S. Expression of Musashi-1 in human normal colon crypt cells: a possible stem cell marker of human colon epithelium. Dig Dis Sci 2003;48:1523–9.
12. Pastò A, Marchesi M, Diamantini A, Frasson C, Curtarello M, Lago C, et al. PKH26 staining defines distinct subsets of normal human colon epithelial cells at different maturation stages. PLoS ONE 2012;7:e43379.

13. Serafin V, Persano L, Moserle L, Esposito G, Ghisi M, Curtarello M, et al. Notch3 signalling promotes tumour growth in colorectal cancer. J Pathol 2011;224:448–60.
14. Fan LF, Dong WG, Jiang CQ, Xia D, Liao F, Yu QF. Expression of putative stem cell genes Musashi-1 and beta1-integrin in human colorectal adenomas and adenocarcinomas. Int J Colorectal Dis 2010;25:17–23.
15. Drewinko B, Romsdahl MM, Yang LY, Ahearn MJ, Trujillo JM. Establishment of a human carcinoembryonic antigen-producing colon adenocarcinoma cell line. Cancer Res1976;36:467–75.
16. Dalerba P, Guiducci C, Poliani PL, Cifola I, Parenza M, Frattini M, et al. Reconstitution of human telomerase reverse transcriptase expression rescues colorectal carcinoma cells from *in vitro* senescence: evidence against immortality as a constitutive trait of tumor cells. Cancer Res 2005;65:2321–9.
17. Indraccolo S, Minuzzo S, Masiero M, Pusceddu I, Persano L, Moserle L, et al. Cross-talk between tumor and endothelial cells involving the Notch3-Dll4 interaction marks escape from tumor dormancy. Cancer Res 2009;69:1314–23.
18. Rothe C, Urlinger S, Lohning C, Prassler J, Stark Y, Jager U, et al. The human combinatorial antibody library HuCAL GOLD combines diversification of all six CDRs according to the natural immune system with a novel display method for efficient selection of high-affinity antibodies. J Mol Biol 2008;376:1182–200.
19. Chadwick N, Zeef L, Portillo V, Fennessy C, Warrander F, Hoyle S, et al.I dentification of novel Notch target genes in T cell leukaemia. Mol Cancer 2009;8:35.
20. Williams CK, Li JL, Murga M, Harris AL, Tosato G. Up-regulation of the Notch ligand Delta-like 4 inhibits VEGF-induced endothelial cell function. Blood2006;107:931–9.
21. Indraccolo S, Gola E, Rosato A, Minuzzo S, Habeler W, Tisato V, et al. Differential effects of angiostatin, endostatin and interferon-alpha(1) gene transfer on *in vivo* growth of human breast cancer cells. Gene Ther 2002;9:867–78.
22. Bertotti A, Migliardi G, Galimi F, Sassi F, Torti D, Isella C, et al. A molecularly annotated platform of patient-derived xenografts ("xenopatients") identifies HER2 as an effective therapeutic target in cetuximab-resistant colorectal cancer. Cancer Discov2011;1:508–23.
23. Galimi F, Torti D, Sassi F, Isella C, Cora D, Gastaldi S, et al. Genetic and expression analysis of MET, MACC1, and HGF in metastatic colorectal cancer: response to met inhibition in patient xenografts and pathologic correlations. Clin Cancer Res2011;17:3146–56.
24. Agnusdei V, Minuzzo S, Frasson C, Grassi A, Axelrod F, Satyal S, et al. Therapeutic antibody targeting of Notch1 in T-acute lymphoblastic leukemia xenografts.Leukemia 2013;28:278–88.
25. Mayo C, Lloreta J, Real FX, Mayol X. In vitro differentiation of HT-29 M6 mucus-secreting colon cancer cells involves a trychostatin A and p27(KIP1)-inducible transcriptional program of gene expression. J Cell Physiol 2007;212:42–50.
26. van Es JH, van Gijn ME, Riccio O, van den Born M, Vooijs M, Begthel H, et al. Notch/gamma-secretase inhibition turns proliferative cells in intestinal crypts and adenomas into goblet cells. Nature 2005;435:959–63.
27. Mu X, Isaac C, Greco N, Huard J, Weiss K. Notch Signaling is Associated with ALDH Activity and an Aggressive Metastatic Phenotype in Murine Osteosarcoma Cells.Front Oncol 2013;3:143.
28. Zuurbier L, Homminga I, Calvert V, te Winkel ML, Buijs-Gladdines JG, Kooi C,et al. Notch1 and/or FBXW7 mutations predict for initial good prednisone response but not for improved outcome in pediatric T-cell acute lymphoblastic leukemia patients treated on DCOG or COALL protocols. Leukemia 2010;24:2014–22.
29. Bellavia D, Campese AF, Alesse E, Vacca A, Felli MP, Balestri A, et al. Constitutive activation of NF-kappaB and T-cell leukemia/lymphoma in Notch3 transgenic mice. EMBO J 2000;19:3337–48.
30. Beatus P, Lundkvist J, Oberg C, Lendahl U. The notch 3 intracellular domain represses notch 1-mediated activation through Hairy/Enhancer of split (HES) promoters.Development 1999;126:3925–35.
31. Yamaguchi N, Oyama T, Ito E, Satoh H, Azuma S, Hayashi M, et al. NOTCH3 signaling pathway plays crucial roles in the proliferation of ErbB2-negative human breast cancer cells. Cancer Res 2008;68:1881–8.
32. Park JT, Li M, Nakayama K, Mao TL, Davidson B, Zhang Z, et al. Notch3 gene amplification in ovarian cancer. Cancer Res 2006;66:6312–8.
33. Haruki N, Kawaguchi KS, Eichenberger S, Massion PP, Olson S, Gonzalez A, et al. Dominant-negative Notch3 receptor inhibits mitogen-activated protein kinase pathway and the growth of human lung cancers. Cancer Res 2005;65:3555–61.

34. Beres BJ, George R, Lougher EJ, Barton M, Verrelli BC, McGlade CJ, et al. Numb regulates Notch1, but not Notch3, during myogenesis. Mech Dev 2011;128:247–57.
35. Cambuli FM, Rezza A, Nadjar J, Plateroti M. Musashi1-egfp mice, a new tool for differential isolation of the intestinal stem cell populations. Stem Cells 2013;31:2273–8.
36. Sikandar SS, Pate KT, Anderson S, Dizon D, Edwards RA, Waterman ML, et al. Notch signaling is required for formation and self-renewal of tumor-initiating cells and for repression of secretory cell differentiation in colon cancer. Cancer Res 2010;70:1469–78.
37. Rezza A, Skah S, Roche C, Nadjar J, Samarut J, Plateroti M. The overexpression of the putative gut stem cell marker Musashi-1 induces tumorigenesis through Wnt and Notch activation. J Cell Sci 2010;123:3256–65.
38. Chen X, Thiaville MM, Chen L, Stoeck A, Xuan J, Gao M, et al. Defining NOTCH3 target genes in ovarian cancer. Cancer Res 2012;72:2294–303.
39. Vo DT, Qiao M, Smith AD, Burns SC, Brenner AJ, Penalva LO. The oncogenic RNA-binding protein Musashi1 is regulated by tumor suppressor miRNAs. RNA Biol2011;8:817–28.
40. Chapman G, Liu L, Sahlgren C, Dahlqvist C, Lendahl U. High levels of Notch signaling down-regulate Numb and Numblike. J Cell Biol 2006;175:535–40.
41. Battelli C, Nikopoulos GN, Mitchell JG, Verdi JM. The RNA-binding protein Musashi-1 regulates neural development through the translational repression of p21WAF-1. Mol Cell Neurosci 2006;31:85–96.
42. Huang EH, Hynes MJ, Zhang T, Ginestier C, Dontu G, Appelman H, et al. Aldehyde dehydrogenase 1 is a marker for normal and malignant human colonic stem cells (SC) and tracks SC overpopulation during colon tumorigenesis. Cancer Res2009;69:3382–9.
43. Bu P, Chen KY, Chen JH, Wang L, Walters J, Shin YJ, et al. A microRNA miR-34a-regulated bimodal switch targets notch in colon cancer stem cells. Cell Stem Cell2013;12:602–15.
44. Sullivan JP, Spinola M, Dodge M, Raso MG, Behrens C, Gao B, et al. Aldehyde dehydrogenase activity selects for lung adenocarcinoma stem cells dependent on notch signaling. Cancer Res 2010;70:9937–48.